puzzles remain, for example, the reduction of dielectric constant at room temperature by ion removal at 140 °C. The availability of pure α-phase samples and the good separation between α-phase effects at lower temperature and γ-phase effects at higher temperature allow one to distinguish the γ-phase properties even when the sample contains both phases.

The γ-phase films show the very high values of dielectric constant and loss previously reported;[23] single-crystal mats show higher values at lower temperatures even when the apparent γ-phase content is small and most crystals have melted. These samples have high ionic contents, so ac ionic effects might be suspected, even at 10 kHz. However, even higher values were found in material crystallized from the melt in an applied electric field, showing that ions are not required for ϵ' and $\epsilon'' > 100$ at 10 kHz. A cooperative relaxation of the dipoles in the polar γ-phase is required for such a strong relaxation, and it is tempting to describe the high values as the dielectric anomaly of a ferroelectric-to-paraelectric transition. However, the crystals are irreversibly melting at the temperature of the relaxation, and this makes such a description somewhat misleading, even if correct, since the transition from order to disorder is always smeared out in polymer crystals.

Acknowledgment. Financial support by the Cornell Materials Science Center, which is funded by the National Science Foundation, is gratefully acknowledged.

Registry No. (Vinylidene fluoride) (homopolymer), 24937-79-9.

References and Notes

(1) Lovinger, A. J. In "Developments in Crystalline Polymers"; Bassett, D. C., Ed.; Applied Science Publishers: London, 1982.
(2) Ishida, Y.; Watanabe, M.; Yamafuji, Polymers"; **1964**, *200*, 48.
(3) Peterlin, A.; Hollbrook, J. D. *Kolloid Z.* **1965**, *203*, 68.
(4) Koizumi, N.; Yano, S.; Tsunashima, K. *J. Polym. Sci., Part A-2* **1969**, *7*, 59.
(5) Sasabe, H., et al. *J. Polym. Sci., Part A-2* **1969**, *7*, 1405.
(6) Nakagawa, K.; Ishida, Y. *J. Polym. Sci., Polym. Phys. Ed.* **1973**, *11*, 1503.
(7) Yano, S. *J. Polym. Sci. Part A-2* **1970**, *8*, 1057.
(8) Osaki, S.; Uemura, S.; Ishida, Y. *J. Polym. Sci., Part A-2* **1971**, *9*, 585.
(9) Uemura, S. *J. Polym. Sci., Part A-2* **1972**, *10*, 2155.
(10) Yano, S., et al. *J. Polym. Sci., Polym. Phys. Ed.* **1974**, *12*, 1875.
(11) Osaki, S.; Kotaka, T. *Rep. Prog. Polym. Phys. Jpn.* **1980**, *23*, 473.
(12) Uemura, S. *J. Polym. Sci., Polym. Phys. Ed.* **1974**, *12*, 1177.
(13) Hill, N.; Vaughan, W. E.; Price, A. H.; Davies, M. "Dielectric Properties and Molecular Behaviour"; Van Nostrand-Reinhold, London, 1969.
(14) Boyd, R. H. *J. Polym. Sci., Polym. Phys. Ed.* **1983**, *21*, 493.
(15) Macdonald, J. Ross, *Trans. Faraday Soc.* **1971**, *66*, 943.
(16) Macdonald, J. Ross, *J. Chem. Phys.* **1971**, *54*, 2026.
(17) Miyamoto, Y.; Miyaji, H.; Asai, K. *Rep. Prog. Polym. Phys. Jpn.* **1977**, *20*, 371.
(18) Miyamoto, Y.; Miyaji, H.; and Asai, K. *J. Polym. Sci., Polym. Phys. Ed.* **1980**, *18*, 597.
(19) Lovinger, A. J. *Polymer* **1980**, *21*, 1317.
(20) Takahashi, Y.; Matsubara, Y.; and Tadokoro, H., *Macromolecules* **1982**, *15*, 334.
(21) Osaki, S.; Kotaka, T. *Ferroelectrics* **1981**, *32*, 1.
(22) Osaki, S.; Ishida, Y. *J. Polym. Sci., Polym. Phys. Ed.* **1975**, *13*, 1071.
(23) Osaki, S.; Ishida, Y.; Yamufuji, K. *Polym. J.* **1980**, *12*, 171.
(24) Takahashi, N.; Odajima, A. *Ferroelectrics* **1981**, *32*, 49.
(25) Furakawa, T., et al. *Ferroelectrics* **1981**, *32*, 61.
(26) Tashiro, K., et al. *Polymer* **1983**, *24*, 199.
(27) Nakagawa, K.; Ishida, Y. *J. Polym. Sci., Polym. Phys. Ed.* **1973**, *11*, 2153.
(28) Choi, K. W. M. S. Thesis, Cornell University, 1981.
(29) Grubb, D. T.; Choi, K. W. *J. Appl. Phys.* **1981**, *52*, 5908.
(30) Weinhold, S.; Lando, J. B.; Litt, M. H. Proceedings of the 11th NATAS Conference, Oct 18–21, 1981.
(31) Osaki, S.; Uemura, S.; and Ishida, Y. *Rep. Prog. Polym. Phys. Jpn.* **1970**, *13*, 403.
(32) Oka, Y.; Koizumi, N. *Polym. J.* **1982**, *14*, 869.
(33) Uchidoi, M., et al. *Rep. Prog. Polym. Phys. Jpn.* **1979**, *22*, 345.
(34) Wunderlich, B. "Macromolecular Physics"; Academic Press: New York, 1978; Vol. 2.
(35) Lovinger, A. J., et al. *Bull. Am. Phys. Soc.* **1983**, *28*, 577.
(36) Prest, W., Jr.; Luca, D. J. *J. Appl. Phys.* **1975**, *46*, 4136.

Dielectric Relaxations and Molecular Motions in Homopolymers and Copolymers of Vinylidene Fluoride and Trifluoroethylene

T. Furukawa,[*1a] **M. Ohuchi,**[1b] **A. Chiba,**[1b] **and M. Date**[1a]

The Institute of Physical and Chemical Research, Wako, Saitama 351, Japan, and Waseda University, Shinjuku, Tokyo 160, Japan. *Received September 13, 1983*

ABSTRACT: The complex dielectric constant has been measured for homopolymers and copolymers of vinylidene fluoride (VDF) and trifluoroethylene (TrFE) over the frequency range of 1 Hz to 100 MHz at temperatures between −100 and +140 °C. The copolymers show dielectric relaxations associated with a ferroelectric-to-paraelectric phase transition in the crystalline regions. The transition point T_c upon cooling is located near 70 °C. The VDF-rich copolymers show thermal hysteresis in that T_c upon heating is much higher than that upon cooling. Near T_c, the relaxation strength $\Delta\epsilon$ becomes a maximum and the relaxation time τ shows a shoulder. These anomalies and hysteresis are removed by taking the ratio of τ to $\Delta\epsilon$ (the kinetic coefficient) following an Arrhenius-type temperature dependence throughout the transition region. The transition causes changes in the equilibrium permittivity but does not affect the kinetic coefficient. The Arrhenius form of the kinetic coefficient extends well below room temperature, where the noncrystalline relaxation is dominant. This relaxation is analogous to the local relaxation in the TrFE homopolymer but contrasts with the primary relaxation in the VDF homopolymer in the context that the former is of an Arrhenius type while the latter is of a WLF type. It is concluded that the noncrystalline and the ferroelectric relaxations of the copolymers arise from the same type of molecular motions, which basically consist of cooperative trans–gauche transformations.

Introduction

The copolymer of vinylidene fluoride (VDF) with trifluoroethylene (TrFE) has attracted much interest recently because it undergoes a ferroelectric-to-paraelectric phase transition. The transition has been reported to be accompanied by an abrupt increase in crystal lattice spacing, a large increase in dielectric constant, loss of remanent polarization, and an endothermic DSC peak.[2-4] Recent investigations[5-8] have shown that the transition is primarily accomplished by intramolecular conformational changes.

Dielectric relaxations have previously been investigated in the 55/45 and 65/35 copolymers[9,10] revealing the kinetic

0024-9297/84/2217-1384$01.50/0

character. Related motions have been shown to be cooperative because of anomalous temperature dependence of the relaxation strength and the relaxation time near the transition point. In this paper, we extend the previous work to the entire range of copolymers, including VDF and TrFE homopolymers, and investigate molecular motions associated with both crystalline and noncrystalline regions.

Experimental Section

The samples of poly(trifluoroethylene) (PTrFE) and the VDF/TrFE copolymers were supplied by Daikin Kogyo Co., Ltd., Japan and those of poly(vinylidene fluoride) (PVDF) by Kureha Chemicals Co., Ltd., Japan. The molar fractions of VDF/TrFE copolymers were 13/87, 37/63, 52/48, 65/35, 73/27, and 82/18. PTrFE and copolymers were cast from methyl ethyl ketone or acetone to obtain 50–100-μm-thick films. Films of PVDF were obtained by crystallization from the melt. Circular gold electrodes 2 cm in diameter were vacuum deposited onto both surfaces of samples.

The complex dielectric constant $\epsilon = \epsilon' - i\epsilon''$ was measured over the frequency range of 1 Hz to 100 MHz at temperatures between −100 and +140 °C. An automatically balancing bridge developed by the authors[11] was used for the measurement at low frequencies between 1 and 100 Hz, an impedance analyzer (Type 4192A, Yokogawa-Hewlett-Packard) at medium frequencies between 100 Hz and 10 MHz, and a vector voltmeter (Type 8405A, Hewlett-Packard) at high frequencies between 10 and 100 MHz. The results above 1 MHz were corrected by taking into consideration the effect of conductance and inductance of the sample cell and leads. Before the measurement, the samples were annealed at 140 °C for 1 h in a sample cell filled with dry nitrogen gas. Measurements were also done in the nitrogen environment.

Results

A. Temperature Dispersion. Parts a and b of Figure 1 show plots of ϵ' and ϵ'' at 1 kHz as a function of temperature for all samples investigated. Two prominent relaxations are observed near −20 and +70 °C. The low-temperature process in PVDF has been ascribed to the micro-Brownian motions of molecular segments in the noncrystalline regions.[12,13] The incorporation of TrFE results in a lower and broader ϵ'' peak. The low-temperature processes in the copolymers and PTrFE may also be ascribed to the noncrystalline regions, although their characteristics are quite different from those in PVDF as will be shown later.

The high-temperature processes characteristic of the ϵ' peak in the copolymers are related to the ferroelectric transition. The 65/35 and 73/27 copolymers reveal thermal hysteresis in that the transition temperature upon heating (dashed line) is much higher than that upon cooling (solid line). When the VDF content exceeds 80%, the transition is obscurred by melting. In the similar temperature range, PVDF exhibits a crystalline relaxation[12–14], in the α phase.

B. Frequency Dispersion. A more thorough analysis of the relaxation process is obtained by measuring the frequency dependence of ϵ' and ϵ''. We first show in Figures 2 and 3 results on PVDF and PTrFE, respectively, which are consistent with earlier publications.[12–16] In PVDF, we can observe two separate relaxations at high and low frequencies corresponding respectively to the low- and high-temperature processes indicated in Figure 1b. On the other hand, PTrFE exhibits only a single ϵ'' peak whose height rapidly increases with increasing temperature.

The copolymers exhibit a single ϵ'' peak analogous to PTrFE. Figure 4 shows results on the 37/63 copolymer. The low and broad peak of ϵ'' at −20 °C becomes higher and sharper with increasing temperature. The value of ϵ' at low frequencies thereby increases rapidly until 80 °C is reached and then decreases. The sharp changes of ϵ' and ϵ'' near 80 °C indicate the occurrence of a ferroelectric phase transition in the crystalline regions. It is noted that the high- and low-temperature processes observed in Figure 1 are not separable in the frequency domain.

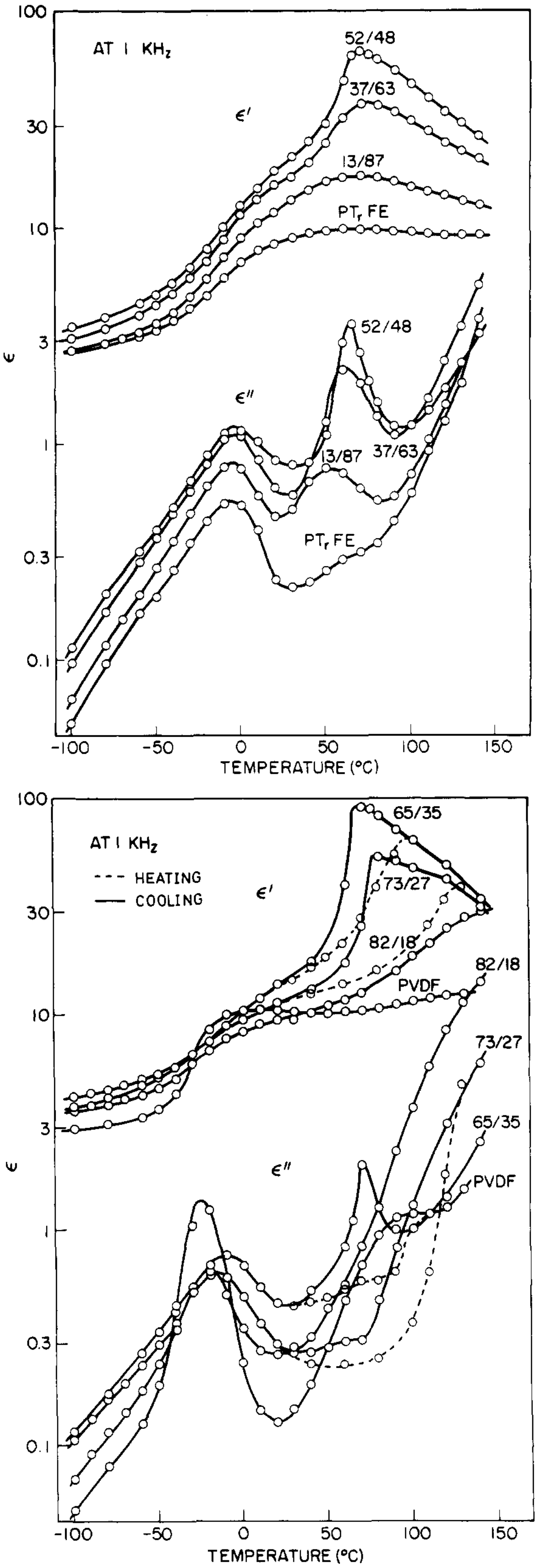

Figure 1. (a) Temperature dependence of ϵ' and ϵ'' at 1 kHz for PTrFE and the 13/87, 37/63, and 52/48 copolymers. (b) Temperature dependence of ϵ' and ϵ'' at 1 kHz for the 65/35, 73/27, and 82/18 copolymers and PVDF.

As the VDF content exceeds 50%, the ferroelectric relaxation reveals itself more dramatically. Figure 5 shows

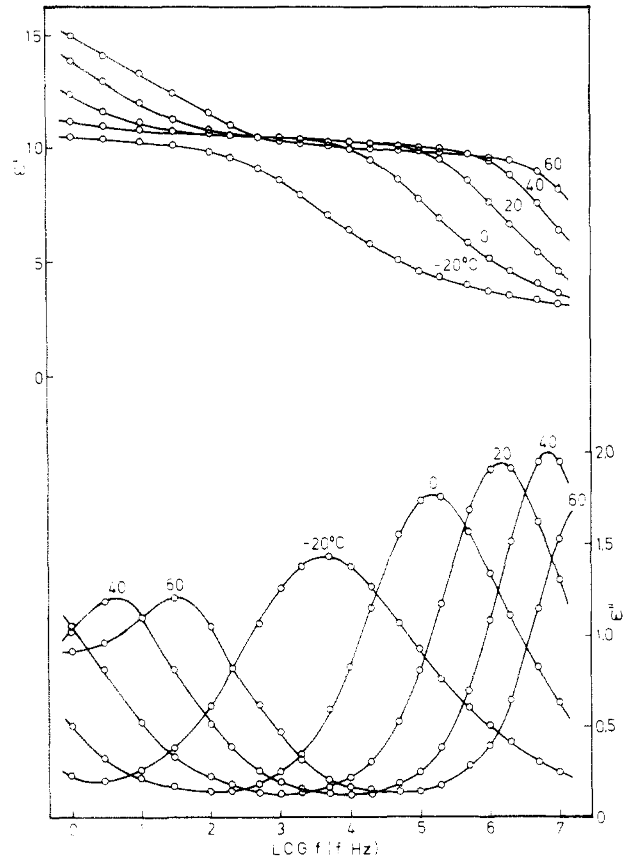

Figure 2. Frequency dependence of ϵ' and ϵ'' for PVDF.

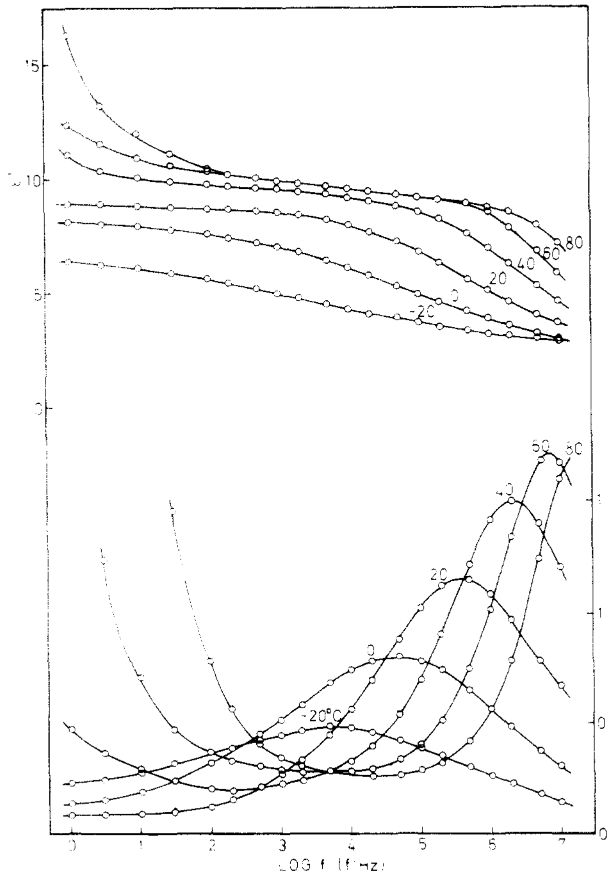

Figure 3. Frequency dependence of ϵ' and ϵ'' for PTrFE.

results on the 65/35 copolymer obtained during heating. Changes in the ϵ'' peak height and the ϵ' low-frequency value with temperature are extremely remarkable near 100 °C. Because of thermal hysteresis, such changes occur near 70 °C during cooling.

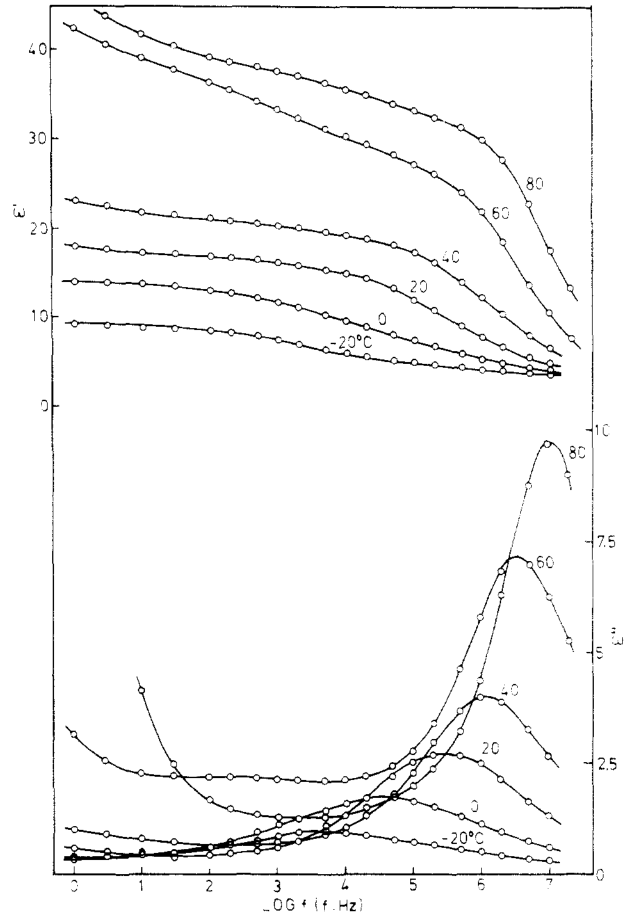

Figure 4. Frequency dependence of ϵ' and ϵ'' for the 37/63 copolymer.

C. Relaxation Time. The relaxation time τ is determined from the ϵ'' peak frequency f_m by the equation

$$\tau = 1/2\pi f_m \quad (1)$$

Parts a and b of Figure 6 show plots of the logarithm of τ against the reciprocal of absolute temperature $1/T$. We find that all samples except PVDF give single continuous curves which show a deflection near -20 °C and a shoulder at 70–120 °C. In the 65/35 and 73/27 copolymers, τ takes different values during heating and cooling. PVDF gives two separate curves. The low-temperature process associated with the segmental motions in the noncrystalline regions exhibits a WLF-type temperature dependence of τ. The high-temperature process associated with crystalline motions in the α phase is of an Arrhenius type with an activation energy of 20 kcal/mol. PTrFE gives a single straight line. This process has been ascribed[15,16] to local motions of noncrystalline molecules rather than to large-scale segmental motions.

D. Relaxation Strength. The conventional Cole–Cole plot of ϵ' and ϵ'' on the complex plane allows the evaluation of the equilibrium dielectric constant $\epsilon(0)$ and the instantaneous dielectric constant $\epsilon(\infty)$. Results show that $\epsilon(0)$ depends strongly upon temperature while $\epsilon(\infty)$ is 3–4, being independent of temperature. Figure 7 shows the temperature dependence of the relaxation strength defined by

$$\Delta\epsilon = \epsilon(0) - \epsilon(\infty) \quad (2)$$

The copolymers and PTrFE show a rapid increase in $\Delta\epsilon$ with increasing temperature near -30 °C, corresponding

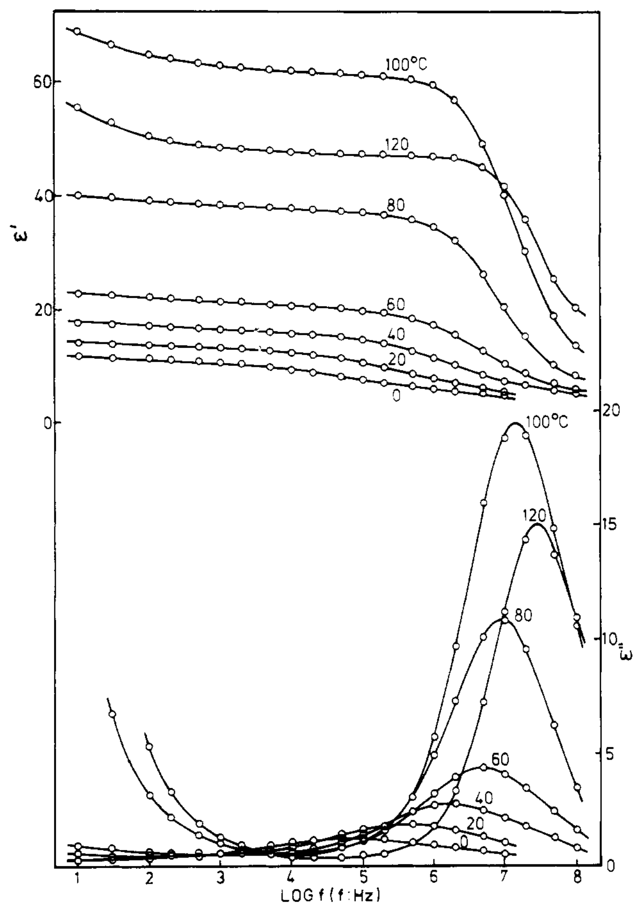

Figure 5. Frequency dependence of ε' and ε'' for the 65/35 copolymer during heating.

to the deflection of the log τ vs. 1/T curve in Figure 6. Near 70 °C, Δε becomes a maximum, corresponding to the shoulder in the log τ vs. 1/T curve. The Δε maximum temperature defines the ferroelectric transition point T_c. The 65/35 and 73/27 copolymers have different T_c values during heating and cooling. In Figure 7, we have tentatively drawn near 0 °C dashed lines separating high- and low-temperature processes. With respect to PVDF, open circles indicate Δε of the primary relaxation and filled circles indicate additional contribution from the crystalline relaxation.

Ferroelectric Relaxation

PVDF[17] is known to crystallize from the melt into the nonpolar α phase, adopting a TGT$\bar{G}$ conformation. The polar all-trans β phase, which is responsible for its ferroelectricity, is usually obtained by uniaxial drawing of the α-phase sample. Incorporation of a small amount of TrFE has been shown[18] to favor direct crystallization into the β phase. On the other hand, PTrFE is believed to crystallize into the nonpolar phase consisting of 3/1-helical molecules and their hexagonal packing.[19] Therefore increasing TrFE content must induce either continuous or discontinuous changes in crystalline structures from an all-trans phase to a 3/1-helical phase. Actually the 52/48 copolymer is shown to exist in a mixture of all-trans and disordered helical phases at room temperature.[5,6]

Dielectric investigations presented here have shown that all copolymers containing 13–73 mol % VDF undergo a ferroelectric-to-paraelectric transition by revealing a maximum of Δε. Figure 8 shows plots of the transition point T_c and the $\Delta\epsilon_{max}$ value as a function of VDF content. The melting point T_m taken from Yagi's paper[4] is also plotted in the figure. It is seen that T_c upon cooling is located near 70 °C for all copolymers investigated. When the VDF content exceeds 65 mol %, T_c upon heating rapidly shifts to higher temperature and finally coalesces

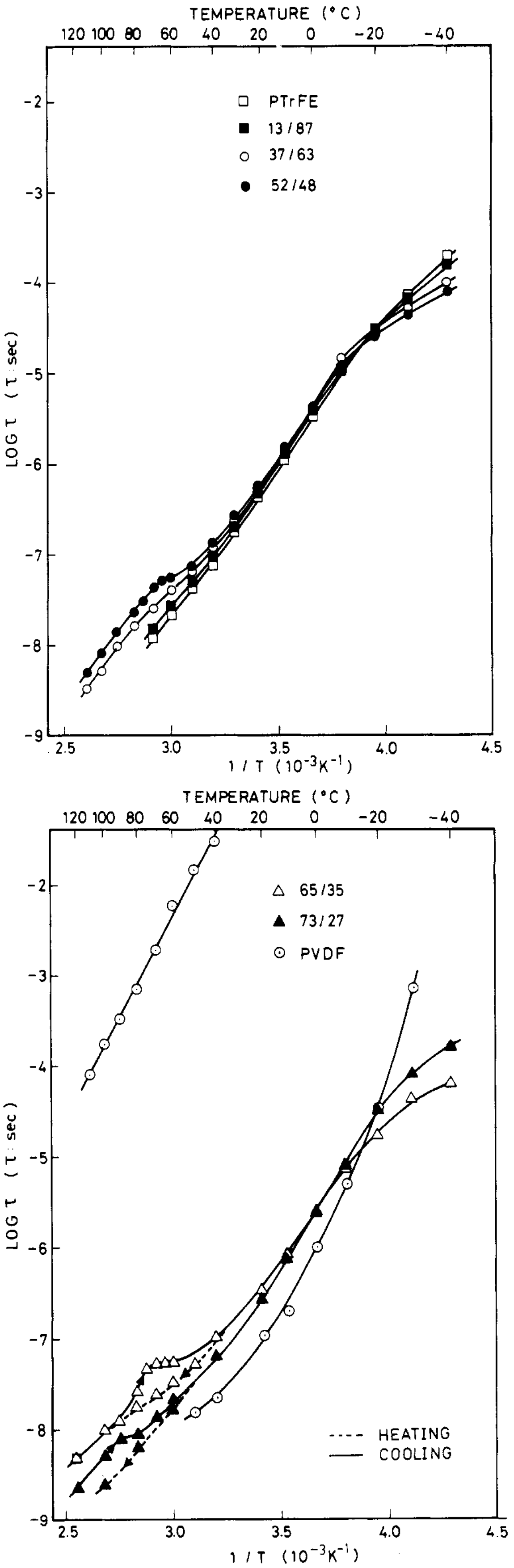

Figure 6. (a) Plots of log τ vs. 1/T for PTrFE and the 13/87, 37/63, and 52/48 copolymers. (b) Plots of log τ vs. 1/T for the 65/35 and 73/27 copolymers and PVDF.

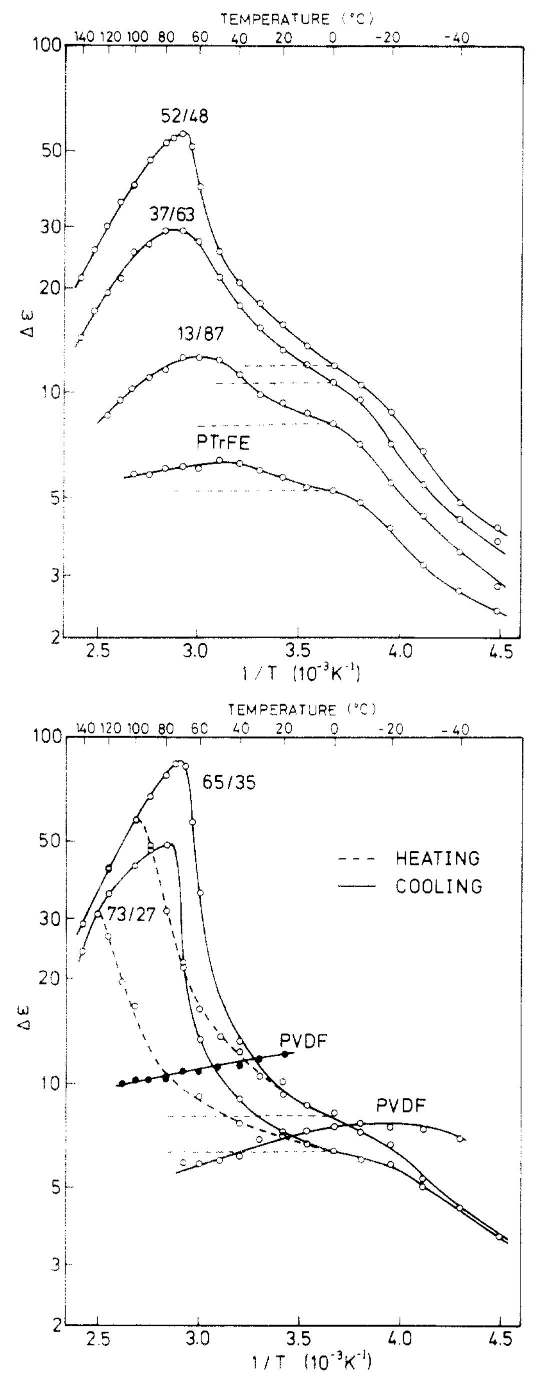

Figure 7. (a) Plots of $\Delta\epsilon$ vs. $1/T$ for PTrFE and the 13/87, 37/63, and 52/48 copolymers. (b) Plots of $\Delta\epsilon$ vs. $1/T$ for the 65/35 and 73/27 copolymers and PVDF.

with T_m. It has been shown[7] that the 78/22 copolymer, which entirely consists of an all-trans phase, starts melting before the completion of the transition. The existence of a small amount of gauche segments seems to be necessary to trigger the transition.

Extrapolation to 100% VDF in Figure 8 predicts T_c upon heating to be ca. 200 °C,[7] which is above the melting point 190 °C of pressure-crystallized β-PVDF.[20] Actually, we have observed no ferroelectric transition in our melt-crystallized α-PVDF. The nonpolar α phase is more stable than the β phase at an atmospheric pressure for the copolymer with the VDF content larger than 90%. We have observed only the crystalline relaxation at 40–100 °C which is characteristic of α-PVDF and quite different from the ferroelectric relaxation in terms of the relaxation time and strength. Miyamoto et al.[14] have proposed a model for this relaxation in that changes in the dipole moment of $TGT\bar{G}$ molecules occur along the chain direction as a result of conformational changes.

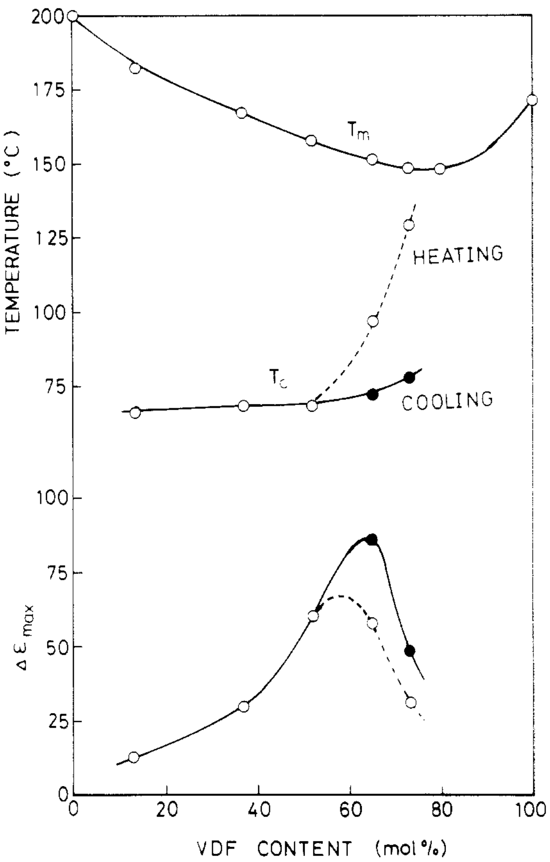

Figure 8. Plots of the melting temperature T_m, the transition temperature T_c, and the maximum relaxation strength $\Delta\epsilon_{max}$ against the VDF content.

As shown in the previous paper,[10] the ferroelectric relaxation can be discussed on the basis of phenomenological theory, which starts with the dielectric equation of state at its equilibrium

$$E = \beta(T - T_0)P + \xi P^3 + \zeta P^5 \qquad (3)$$

where E is the electric field and P is the polarization. The coefficients β and ζ are positive and ξ can be positive or negative, depending upon the order of the transition. T_0 is the temperature where the linear coefficient changes its sign. This equation gives the spontaneous polarization P_s in the ferroelectric phase by solving for P at $E = 0$. The zero-field reciprocal permittivity χ is derived by differentiating E with respect to P

$$\chi = \beta(T - T_0) + 3\xi P_s^2 + 5\zeta P_s^4 \qquad (4)$$

At the ferroelectric transition point, χ undergoes either a discontinuous or a continuous change, depending upon the order of the transition due to loss or creation of P_s.

The nonequilibrium and relaxational dielectric equation turns out to be

$$\gamma\delta\dot{P} + \chi\delta P = \delta E \qquad (5)$$

where γ is the kinetic coefficient expressing the resistance against a change in δP with time. This equation is solved to obtain

$$\delta P = \frac{1}{\chi + i\omega\gamma}\delta E \qquad (6)$$

where ω is the angular frequency. Comparison with an expression for the relative dielectric constant

$$\epsilon = \epsilon(\infty) + \frac{\Delta\epsilon}{1 + i\omega\tau} \qquad (7)$$

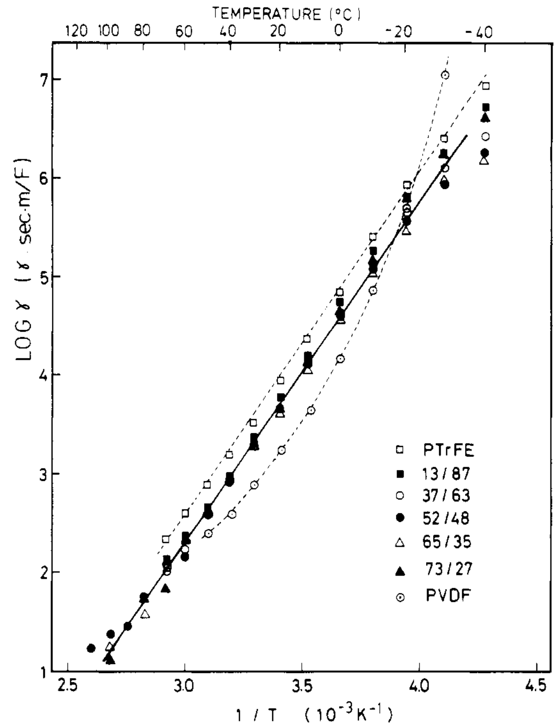

Figure 9. Plots of the kinetic coefficients against $1/T$ for homopolymers and copolymers of VDF and TrFE.

gives relations between experimental quantities ($\Delta\epsilon$ and τ) and the phenomenological coefficients (γ and χ) as follows:

$$\epsilon_0 \Delta\epsilon = 1/\chi \quad (8)$$

$$\tau = \gamma/\chi \quad (9)$$

Here ϵ_0 is the dielectric constant of free space.

By eq 8, $\Delta\epsilon$ is simply related to the reciprocal of χ. Thus the observed peak of $\Delta\epsilon$ is ascribed to the minimum of χ at T_c. On the other hand, τ reflects the temperature dependence of both γ and χ. We then calculated γ by the equation

$$\gamma = \tau/\epsilon_0\Delta\epsilon \quad (10)$$

and the result is shown in Figure 9. It is seen that γ of all copolymers lies on a single straight line given by an Arrhenius form

$$\gamma = \gamma_0 \exp(\Delta U/RT) \quad (11)$$

with an activation energy ΔU of 16 kcal/mol. This means that the potential barrier for related molecular motions does not change its height as a result of the phase transition. The shoulder and hysteresis in τ are completely removed in γ.

Figure 10 schematically represents the temperature dependence of experimental and phenomenological coefficients. Here we have assumed that the transition is of a first order. Thus χ undergoes a jump at T_c while log γ is linearly proportional to $1/T$. From eq 8 and 9, $\Delta\epsilon$ and log τ are expected to show jumps at T_c. Actually, $\Delta\epsilon$ have exhibited a peak and log τ a shoulder as shown by dashed lines in Figure 10 due probably to a distribution in T_c inherent to the polycrystalline structure of the polymeric substances.

The ferroelectric phase basically consists of all-trans molecules and the paraelectric phase consists of random TT, TG, and T$\bar{\text{G}}$ sequences, which are simply called disordered helices.[5,6] The most important finding in our results is that the height of the potential barrier is invariant below and above T_c. Figure 11a shows a schematic drawing of proposed crystalline structures of the VDF–TrFE copolymer. We assume that the ferroelectric phase more or less contains disordered helical segments and the paraelectric phase short all-trans segments. In these structures, we can expect such thermal fluctuations that a certain number of trans segments cooperatively transform into disordered helical conformations and vice versa at the boundary of all-trans and disordered helical segments. Since such motions basically occur intramolecularly, we may obtain an Arrhenius type of γ with an invariant potential barrier below and above T_c. As shown in Figure 11b, the electric field may induce growth or diminution of all-trans segments, depending upon whether the field is parallel or antiparallel to the direction of dipoles in all-trans segments.

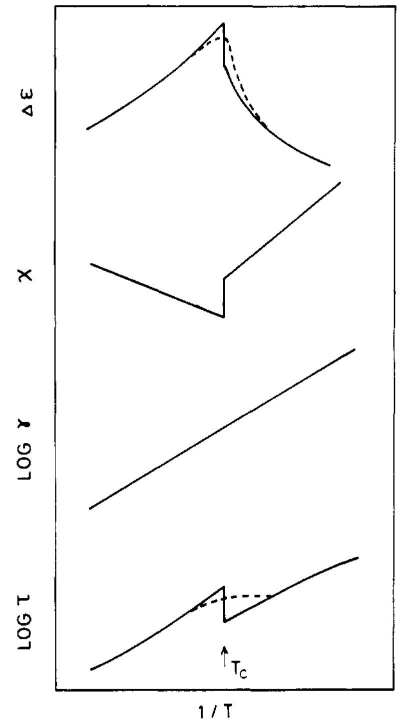

Figure 10. Temperature dependence of experimental coefficients ($\Delta\epsilon$ and τ) and phenomenological coefficients (χ and γ) near T_c.

The relaxation strength may be proportional to the number of boundary regions. As shown in Figure 8, the 65/35 copolymer has the largest $\Delta\epsilon_{\max}$ value. The decreasing VDF content above 65 mol % favors disordered helical conformations while the increasing VDF content favors an all-trans conformation. The 65/35 copolymer seems to contain an optimum fraction of all-trans and disordered helical segments, resulting in the largest number of boundary regions.

Noncrystalline Relaxations

In Figure 9, we see that the linear relationship between log γ and $1/T$ extends well below room temperature, where crystalline motions are almost frozen-in and noncrystalline motions are dominant. Dashed lines in Figure 9 indicate the kinetic coefficients of PVDF and PTrFE associated with primary and local relaxations in the noncrystalline regions. Since $\Delta\epsilon$ of PVDF shows only a weak temperature dependence, the WLF form of τ is preserved in γ. It is interesting to note that the WLF-type temperature dependence of τ in PVDF near the glass transition point arises from an increase in the resistance or the viscosity (kinetic term) whereas an anomaly in τ near the ferroelectric transition point of the VDF–TrFE copolymers originates from the equilibrium permittivity (static term).

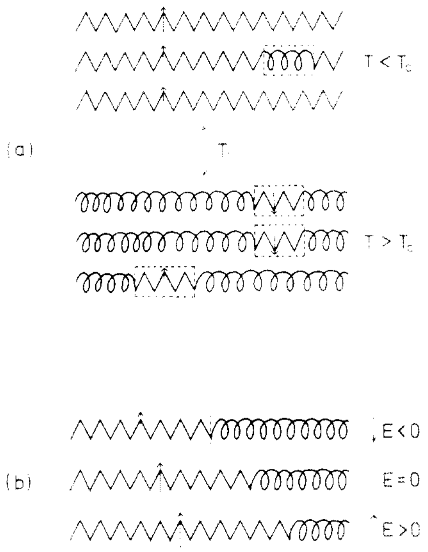

Figure 11. Schematic drawing of crystalline structures of the VDF–TrFE copolymers below and above T_c (a) and possible conformational changes induced by the electric field (b).

The noncrystalline relaxation in the VDF–TrFE copolymers is analogous to that in PTrFE. The dielectric relaxation in PTrFE has been ascribed to some local motions because of strong temperature dependence of $\Delta\epsilon$ and the Arrhenius-type temperature dependence of τ. The glass transition of PTrFE has been considered to exist near 50 °C, where a strong mechanical relaxation is observed.[15,16]

That the noncrystalline and ferroelectric relaxations of the copolymers show the same temperature dependence of γ leads us to conclude that both processes arise from the same type of molecular motions. We consider that there exist short all-trans segments even in the noncrystalline regions. Since molecular motions as shown in Figure 11 are basically local, such motions can also take place in the noncrystalline regions.

At the moment, there remains a question about the location of the glass transition point T_g of the copolymers. One of the possibilities is that the noncrystalline relaxation observed is associated with T_g but for some reason we have obtained τ of an Arrhenius type rather than of a WLF type. The other is that there exists T_g at higher temperature. But since the noncrystalline relaxation has already resulted in fairly large $\Delta\epsilon$, the onset of segmental motions has not resulted in additional $\Delta\epsilon$.

Conclusions

The VDF–TrFE copolymers exhibit two dielectric relaxations associated the noncrystalline and the crystalline regions. These relaxations are inseparable in a frequency domain because the relaxation times for respective processes are identical or very close. The noncrystalline relaxation becomes active near −30 °C and results in $\Delta\epsilon$ of ca. 5. The crystalline relaxation is related with the ferroelectric phase transition occurring above 70 °C and results in much larger $\Delta\epsilon$ up to 85. Near T_c, $\Delta\epsilon$ becomes a maximum and τ shows a shoulder. The ratio $\tau/\epsilon_0\Delta\epsilon$ corresponding to the kinetic coefficient follows an Arrhenius-type temperature dependence from −30 to +120 °C, indicating that the potential barrier for crystalline and noncrystalline motions is identical and is not affected by structural changes. Possible molecular motions responsible for these relaxations are ascribed to cooperative trans–gauche transformations at the boundary between all-trans and disordered helical segments.

Acknowledgment. We thank Mr. J. Sako of Daikin Kogyo Co. and Mr. K. Nakamura of Kureha Chemicals Co. for provision of samples.

References and Notes

(1) (a) The Institute of Physical and Chemical Research. (b) Waseda University.
(2) Furukawa, T.; Johnson, G. E.; Bair, H. E.; Tajitsu, Y.; Chiba, A.; Fukada, E. *Ferroelectrics* **1981**, *32*, 61.
(3) Yamada, T.; Ueda, T.; Kitayama, T. *J. Appl. Phys.* **1981**, *52*, 948.
(4) Yagi, T.; Tatemoto, M.; Sako, J. *Polym. J.* **1980**, *12*, 209.
(5) Lovinger, A. J.; Davis, G. T.; Furukawa, T.; Broadhurst, M. G. *Macromolecules* **1982**, *15*, 329.
(6) Davis, G. T.; Furukawa, T.; Lovinger, A. J.; Broadhurst, M. G. *Macromolecules* **1982**, *15*, 329.
(7) Lovinger, A. J.; Furukawa, T.; Davis, G. T.; Broadhurst, M. G. *Polymer* **1983**, *24*, 1225, 1233.
(8) Tashiro, K.; Takano, K.; Kobayashi, M.; Chatani, Y.; Tadokoro, H. *Polymer* **1981**, *22*, 1312.
(9) Furukawa, T.; Johnson, G. E. *J. Appl. Phys.* **1981**, *52*, 940.
(10) Ohuchi, M.; Chiba, A.; Date, M.; Furukawa, T. *Jpn. J. Appl. Phys.* **1983**, *22*, 1267.
(11) Furukawa, T.; Fukada, E. *J. Polym. Sci.* **1976**, *14*, 1979.
(12) Sasabe, H.; Saito, S.; Asahina, M.; Kakutani, H. *J. Polym. Sci.* **1969**, *7*, 1405.
(13) Yano, S. *J. Polym. Sci.* **1970**, *8*, 1057.
(14) Miyamoto, Y.; Miyaji, H.; Asai, K. *J. Polym. Sci., Polym. Phys. Ed.* **1980**, *18*, 597.
(15) Choy, C. L.; Tse, T. K.; Tsui, S. M.; Hsu, B. S. *Polymer* **1975**, *16*, 501.
(16) Yagi, T. *Polym. J.* **1979**, *9*, 711.
(17) Hasegawa, R.; Takahashi, Y.; Chatani, Y.; Tadokoro, H. *Polym. J.* **1972**, *3*, 600.
(18) Lando, J. B.; Doll, W. W. *J. Macromol. Sci., Phys.* **1968**, *B2*, 205.
(19) Kolda, R. R.; Lando, J. B. *J. Macromol. Sci., Phys.* **1975**, *B11*, 21.
(20) Matsushige, K.; Takemura, T. *J. Polym. Sci., Phys.* **1980**, *18*, 1665.